Applied Physics Express 2 (2009) 033001

Material Dependence of Thermally Assisted Magnetization Reversal Properties in Microstructured Co/Pd Multilayers

Budi Purnama, Terumitsu Tanaka, Yukio Nozaki, and Kimihide Matsuyama

Department of Electronics, Kyushu University, 744 Motooka, Nishi-ku, Fukuoka 819-0395, Japan

Received December 5, 2008; accepted February 1, 2009; published online February 20, 2009

Using extraordinary Hall resistance (R_H) measurements, the material dependence of thermally assisted magnetization reversal (TAMR) was investigated for microstructured multilayers of [Co (0.17 nm)/Pd (0.80 nm)]$_N$ with $N = 7$ and 20, which exhibit markedly different magnetic properties. The threshold values of the external field ($H_{w,th}$) necessary for controlling the magnetization direction in TAMR, obtained by direct application of a current pulse to the sample, were 220 Oe for the $N = 7$ and 710 Oe for $N = 20$ samples. The values of $H_{w,th}$ are found to be related to the magnetization saturation field at a critical temperature at which apparent coercivity decays.

DOI: 10.1143/APEX.2.033001

Magnetoresistive random access memory (MRAM) is expected to be a universal memory that satisfies the demands for high bit density, fast access time and practically unlimited durability. Thermally assisted magnetization reversal (TAMR) has been proposed for application in MRAM[1–6] as a promising approach to realize the maximum possible bit density using high perpendicular magnetic anisotropy (PMA) materials, as already demonstrated in hard disc drive (HDD) technology. Since the magnetization reversal in MRAM is performed with current-induced local magnetic fields, reduction of the reversal field is essential for low-power memory operation. Unlike conventional magnetization reversal, TAMR is a field-induced magnetic ordering process under significant thermal disturbance. Thus, a threshold value of the external field ($H_{w,th}$) to define the final magnetization direction and its dependence on the material parameters are important for material optimization and the prospects for scaling in thermally assisted MRAM (TA-MRAM). Among the various PMA materials available, Co/Pd multilayers exhibit a wide variety of magnetic properties, including variation in the strength of PMA and its temperature dependence, which can be controlled by varying the individual layer thickness, layer repetition number, and deposition conditions.[7,8] A correlation between the $H_{w,th}$ and the strength of PMA, reflected in the coercivity, was predicted in micromagnetic simulations.[9] The present work compares TAMR performance in microstructured Co/Pd films with different magnetic properties.

Co/Pd multilayers were deposited on glass substrates by tandem-type magnetron sputtering with a multi-cathode system (Anelva SPC-350). Background pressure was below 5.0×10^{-7} Torr, and Ar pressure during deposition was fixed at 20 mTorr. The substrate was mounted on a sample holder and rotated at 50 rpm around the Co and Pd targets using a PC-controlled shutter system. The sputtering rates for Co and Pd were 0.10 and 0.036 nm/s, respectively. Microstructured Co/Pd multilayers with a lateral size of $50 \times 50\,\mu m^2$ were fabricated by photolithography and followed by a lift-off process. Two pairs of 10-μm-wide underlie electrodes of Ti (20 nm)/Au (100 nm), used for Joule heating and extraordinary Hall resistance (R_H) measurements, were fabricated at each edge of the Co/Pd pattern as shown in Fig. 1. In the TAMR experiments, the sample temperature was raised by applying a current pulse to the Co/Pd pattern through one pair of electrodes with a fast pulse generator. The sample resistance was matched to a coaxial cable impedance of 50 Ω with an additional series resistance. A pulse width of 300 ns was chosen, so that the entire structure could attain a thermal stationary state,[10] as was evidenced from the pulse width dependence of TAMR properties. The magnetization reversal behavior was investigated by measuring R_H, which is related to the perpendicular magnetization.[11] The R_H hysteresis for the perpendicular field sweep was also measured at various temperatures with a Cu heat block system. Among the fabricated samples, [Co (0.17 nm)/Pd (0.80 nm)]$_N$ with $N = 7$ and 20, referred to N7 and N20 hereafter, are the focus of the present study since they exhibit significantly different coercivity, which is related to the strength of PMA.

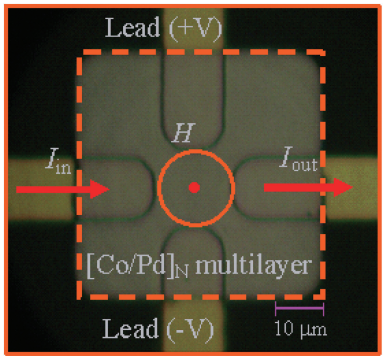

Fig. 1. Schematic top view of microstructured Co/Pd multilayers for TAMR experiments.

Figure 2 shows R_H hysteresis curves for N7 and N20, measured at various temperatures. The plotted R_H values are normalized with that measured at a room temperature (RT) of 23 °C. As can be seen in the figure, superior squareness and remanence are realized for the N7 up to 90 °C, suggesting that the nucleation-type magnetization reversal is dominant at elevated temperatures. In contrast, a gradual increase of R_H without hysteresis is observed at 120 °C, which can be attributed to the enhanced thermal fluctuation effect. Another critical change in the R_H behavior is observed at 190 °C for the sample N20, as shown in Fig. 2(b). The observed hysteresis-free R_H curve with a notable knee is typical of that measured along the effective hard axis direction, which can be explained as follows. The net uniaxial perpendicular anisotropy K_u is a summation of the surface anisotropy ($2K_s/t_{Co}$) and the volume anisotropy

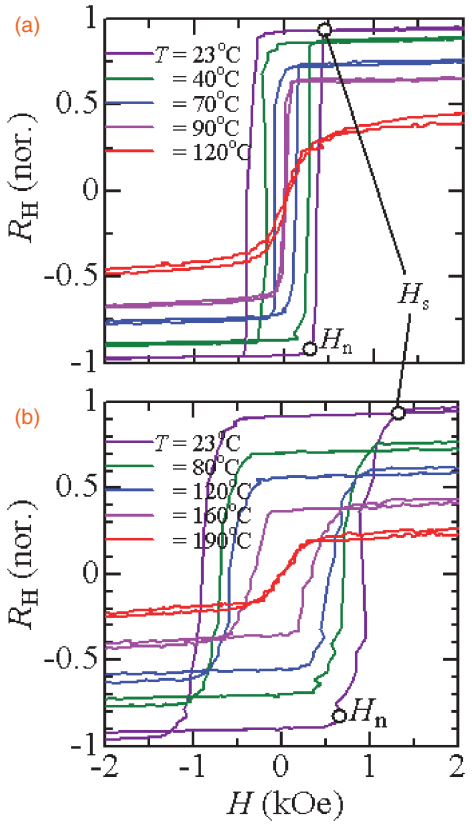

Fig. 2. Hysteresis of extraordinary Hall resistance (R_H) for external field (H) sweep, measured at various temperatures for [Co (0.17 nm)/Pd (0.80 nm)]$_N$ with (a) $N = 7$ and (b) $N = 20$.

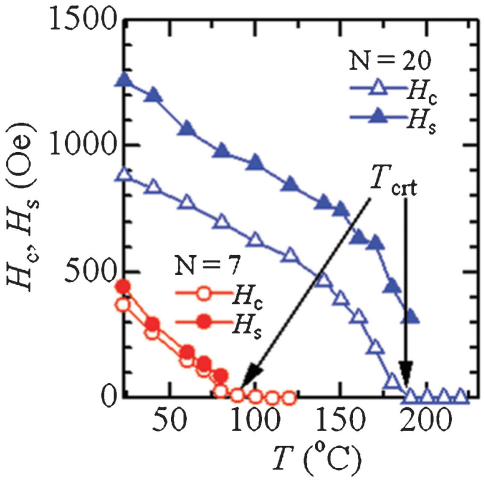

Fig. 3. The temperature dependence of coercive field, H_c and practical saturated field, H_s for [Co (0.17 nm)/Pd (0.80 nm)]$_N$ with $N = 7$ and 20.

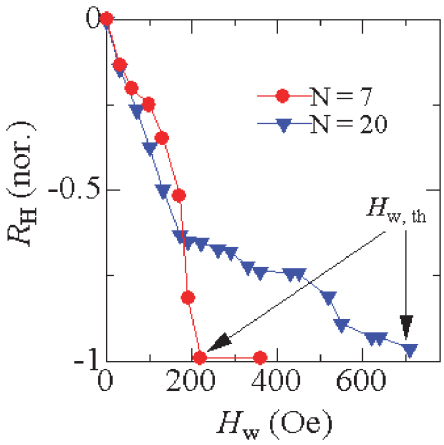

Fig. 4. Extraordinary Hall resistance (R_H) measured after performing TAMR with various external fields (H_w).

(K_v) including the shape anisotropy term.[12] Accordingly, the apparent transition of the effective easy axis direction from perpendicular to in-plane can be caused by the compensation of opposite contributions from K_s and K_v with different temperature dependences. Magnetization reversal is triggered at the nucleation field H_n and is succeeded by wall motion until being practically saturated at H_s, as shown in the figure. The significant difference between H_n and H_s in the case of N20 indicates the significant distribution of intrinsic PMA.[13,14]

Temperature dependences of the coercive field H_c and the saturation field H_s for N7 and N20 are compared in Fig. 3. H_c decreases with the increasing temperature, and decays at a critical temperatures (T_{crt}) of 100 °C for N7 and 190 °C for N20. The thermally demagnetized temperatures, estimated from the temperature dependence of R_H, are 140 °C for N7 and 220 °C for N20, respectively. H_s also decreases with increasing temperature. The different magnetization reversal modes for the two samples are demonstrated in the mostly coincident (N7) and different (N20) values of H_c and H_s for $T < T_{crt}$.

Dynamic TAMR properties have also been investigated by Joule heating with a pulsed conductor current. The experimental procedure is as follows. First the magnetization of the Co/Pd was saturated with a perpendicular field of 4.0 kOe. Thereafter, a current pulse was directly applied through the Co/Pd pattern under various perpendicular fields of H_w. The current amplitude was adjusted so that the normalized R_H after Joule heating becomes zero at $H_w = 0$ Oe, indicating thermal demagnetization. The power densities (p) required for thermal demagnetization are evaluated from the current amplitude as 0.19 mW/μm^2 (N7) and 0.71 mW/μm^2 (N20). The different values of p can be related to the T_{crt} of the two samples.

The values of R_H measured after the above TAMR procedure are shown in Fig. 4 as a function of H_w. R_H decreases with increasing H_w and approaches to the saturation value of about −1 at a threshold field, indicated as $H_{w,th}$ in the figure. $H_{w,th}$ is related to the field strength required to sweep away the domain wall during the field cooling process from the thermally induced demagnetized state. The values of $H_{w,th}$ are 220 Oe for N7 and 710 Oe for N20. These values appear to be correlated with the H_s at raised temperatures, as shown in Fig. 3. The TAMR occurs during the 300-ns-wide current pulse, which is of the order of 10^{-8} shorter than that for the R_H hysteresis measurements (≈30 s). Accordingly, the larger value of $H_{w,th}$ compared with thermally reduced H_s can be attributed to the time dependence of the magnetization reversal field.[15] The marked tail of the R_H–H_w curve for the N20 sample corresponds to the degraded squareness of

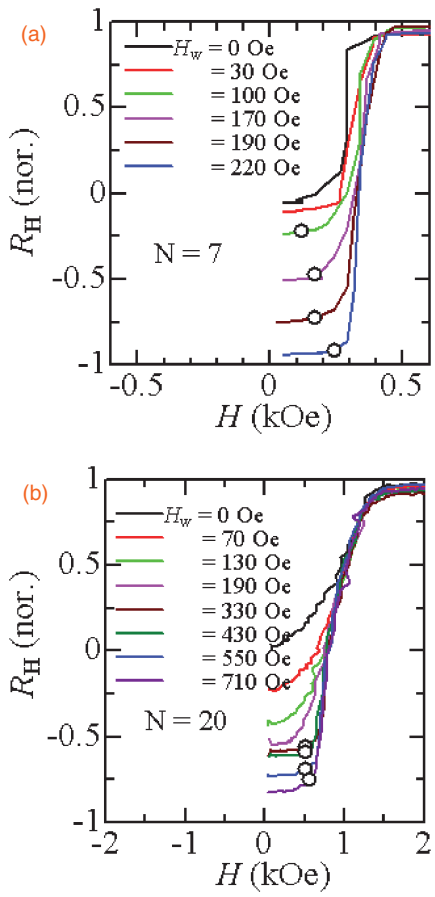

Fig. 5. Extraordinary Hall resistance (R_H) changes with additional field sweep; measured after performing TAMR under various external fields (H_w).

the R_H–H hysteresis, as shown in Fig. 2(b). The gradual decrease of R_H for the N7 sample indicates the stochastic aspect of the wall depinning process in imperfect TAMR, as discussed in the following paragraph. The reduction rate of the field required by the TAMR, defined as $[(H_s(\text{at } 23\,^\circ\text{C}) - H_{w,th})/H_s(\text{at } 23\,^\circ\text{C})]$, is comparable between the two samples; 0.50 for N7 and 0.43 for N20.

To further study TAMR behaviors the evolution of R_H for the integrating field sweep was measured after performing TAMR with various H_w, as shown in Fig. 5. The different R_H–H curves for the two samples also demonstrate the different TAMR properties, originating from individual magnetic characteristics. The rising edge, marked with open circles in the R_H–H curve, indicates the wall depinning field, which increases with increase in H_w and lies closes to the nucleation field, as shown in the figure. This result implies that the domain walls remaining after the imperfect TAMR are trapped at the energy wells, which cannot be overwhelmed by H_w within the cooling time. The gradual increase of R_H for the N20 sample measured at H_w lower than 190 Oe, indicates broad variation in the strength of the wall-trapping energy well. The appearance of the rising edge in the R_H–H curves, notable at H_w larger than 260 Oe, can be explained by the removal of the domain walls with a depinning field smaller than the nucleation field during the TAMR process.

In summary, the material dependence of TAMR behavior has been investigated for microstructured [Co (0.17 nm)/Pd (0.80 nm)]$_N$ patterns with $N = 7$ and 20 using extraordinary Hall effect measurements. Current-induced dynamic Joule heating up to a critical temperature results in about 50% reduction of the reversal field compared with that measured at RT. The threshold value of the external field ($H_{w,th}$) required for controlling the magnetization direction in TAMR was found to be related to the thermally reduced saturation field. That is, the measured $H_{w,th}$ is 220 Oe for $N = 7$ and 710 Oe for $N = 20$. Thus, an optimum design considering for the bit information stability and the magnetization reversal field would be still essential in the TA-MRAM scheme. Further reduction of the reversal field is expected for practical MRAM elements of an order 100 nm or smaller due to the lower demagnetization factor.

1) R. S. Beech, J. A. Anderson, A. V. Pohm, and J. M. Daughton: J. Appl. Phys. **87** (2000) 6403.
2) Z.-H. Wu, S.-H. Lai, S.-H. Huang, and W.-C. Lin: J. Magn. Magn. Mater. **304** (2006) 93.
3) I. L. Prejbeanu, M. Kerekes, R. C. Sousa, O. Redon, B. Dieny, and J. P. Nozieres: J. Phys.: Condens. Matter **19** (2007) 165218.
4) Z.-Y. Liu, G.-C. Han, and Y.-K. Zheng: IEEE Trans. Magn. **40** (2004) 2622.
5) L. You, T. Kato, S. Tsunashima, and S. Iwata: Jpn. J. Appl. Phys. **47** (2008) 146.
6) K.-J. Kim, J.-C. Lee, S.-B. Choe, and K.-H. Shin: Appl. Phys. Lett. **92** (2008) 192509.
7) S. Hashimoto, Y. Ochiai, and K. Aso: J. Appl. Phys. **66** (1989) 4909.
8) B. Purnama, Y. Nozaki, and K. Matsuyama: Dig. Intermag. 2008, HU-08.
9) B. Purnama, Y. Nozaki, and K. Matsuyama: J. Magn. Magn. Mater. **310** (2007) 2683.
10) R. C. Sousa, M. Kerekes, I. L. Prejbeanu, O. Redon, B. Dieny, J. P. Nozieres, and P. P. Freitas: J. Appl. Phys. **99** (2006) 08N904.
11) S. Kim, S. R. Lee, and J. D. Chung: J. Appl. Phys. **73** (1993) 6344.
12) F. J. A. den Broeder, H. C. Donkersloot, H. J. G. Draaisma, and W. J. M. de Jonge: J. Appl. Phys. **61** (1987) 4317.
13) J. W. Lau, R. D. Mcmichael, S. H. Chung, J. O. Rantschler, V. Parekh, and D. Litvinov: Appl. Phys. Lett. **92** (2008) 012506.
14) E. Chunsheng, V. Parekh, P. Ruchhoeft, S. Khizroev, and D. Litvinov: J. Appl. Phys. **103** (2008) 063904.
15) C. S. Brown, J. W. Harrell, and S. Matsunuma: J. Appl. Phys. **100** (2006) 053910.